JOURNAL OF GEOPHYSICAL RESEARCH, VOL. 115, E00E10, doi:10.1029/2009JE003424, 2010

Wet Chemistry experiments on the 2007 Phoenix Mars Scout Lander mission: Data analysis and results

S. P. Kounaves,[1] M. H. Hecht,[2] J. Kapit,[1,3] K. Gospodinova,[1,4] L. DeFlores,[2] R. C. Quinn,[5,6] W. V. Boynton,[7] B. C. Clark,[8] D. C. Catling,[9,10] P. Hredzak,[1] D. W. Ming,[11] Q. Moore,[1] J. Shusterman,[1] S. Stroble,[1] S. J. West,[12] and S. M. M. Young[1]

Received 7 May 2009; revised 31 August 2009; accepted 23 September 2009; published 16 January 2010.

[1] Chemical analyses of three Martian soil samples were performed using the Wet Chemistry Laboratories on the 2007 Phoenix Mars Scout Lander. One soil sample was obtained from the top ~2 cm (Rosy Red) and two were obtained at ~5 cm depth from the ice table interface (Sorceress 1 and Sorceress 2). When mixed with water in a ~1:25 soil to solution ratio (by volume), a portion of the soil components solvated. Ion concentrations were measured using an array of ion selective electrodes and solution conductivity using a conductivity cell. The measured concentrations represent the minimum leachable ions in the soil and do not take into account species remaining in the soil. Described is the data processing and analysis for determining concentrations of seven ionic species directly measured in the soil/solution mixture. There were no significant differences in concentrations, pH, or conductivity, between the three samples. Using laboratory experiments, refinement of the surface calibrations, and modeling, we have determined a pH for the soil solution of 7.7(±0.3), under prevalent conditions, carbonate buffering, and P_{CO2} in the cell headspace. Perchlorate was the dominant anion in solution with a concentration for Rosy Red of 2.7(±1) mM. Equilibrium modeling indicates that measured [Ca^{2+}] at 0.56(±0.5) mM and [Mg^{2+}] at 2.9(±1.5) mM, are consistent with carbonate equilibrium for a saturated solution. The [Na^{+}] and [K^{+}] were 1.4(±0.6), and 0.36(±0.3) mM, respectively. Results indicate that the leached portion of soils at the Phoenix landing site are slightly alkaline and dominated by carbonate and perchlorate. However, it should be noted that there is a 5–15 mM discrepancy between measured ions and conductivity and another species may be present.

Citation: Kounaves, S. P., et al. (2010), Wet Chemistry experiments on the 2007 Phoenix Mars Scout Lander mission: Data analysis and results, *J. Geophys. Res.*, *115*, E00E10, doi:10.1029/2009JE003424.

1. Introduction

[2] The Phoenix Mars Scout Lander set down 25 May 2008 on the partially eroded ejecta blanket ~20 km from the 0.5–0.75 billion year old Heimdal crater, at 68.22°N, 234.25°E (areocentric) [*Smith et al.*, 2009]. The primary scientific goals of the Phoenix were to verify the presence of subsurface ice, understand the history of the water at the landing site, and assess habitability of the site. To meet these goals the Phoenix payload [*Smith et al.*, 2008] included a Thermal and Evolved Gas Analyzer (TEGA), optical (OM) and atomic force microscopes (AFM), a Thermal and Electrical Conductivity Probe (TECP), a robotic arm (RA) with its camera (RAC), a Stereoscopic Surface Imager (SSI), magnetic calibration targets, an atmospheric/weather station (MET), and four identical Wet Chemistry Laboratory (WCL) cells. The goal of the WCLs was to perform a chemical analysis of the solution to which the soil had been added to determine its soluble ionic components, the pH, and the electrical conductivity. From Viking to the MERs, previous landed missions to Mars using elemental measurement techniques have tended to

[1]Department of Chemistry, Tufts University, Medford, Massachusetts, USA.
[2]Jet Propulsion Laboratory, California Institute of Technology, Pasadena, California, USA.
[3]Now at Woods Hole Oceanographic Institution, Woods Hole, Massachusetts, USA.
[4]Now at Department of Mechanical Engineering, Massachusetts Institute of Technology, Cambridge, Massachusetts, USA.
[5]SETI Institute, Moffett Field, California, USA.
[6]NASA Ames Research Center, Moffett Field, California, USA.
[7]Lunar and Planetary Laboratory, University of Arizona, Tucson, Arizona, USA.
[8]Space Science Institute, Boulder, Colorado, USA.
[9]Department of Earth Sciences, University of Bristol, Bristol, UK.
[10]Department of Earth and Space Sciences, University of Washington, Seattle, Washington, USA.
[11]NASA Johnson Space Center, Houston, Texas, USA.
[12]Invensys Process Systems, Foxboro, Massachusetts, USA.

0148-0227/10/2009JE003424$09.00

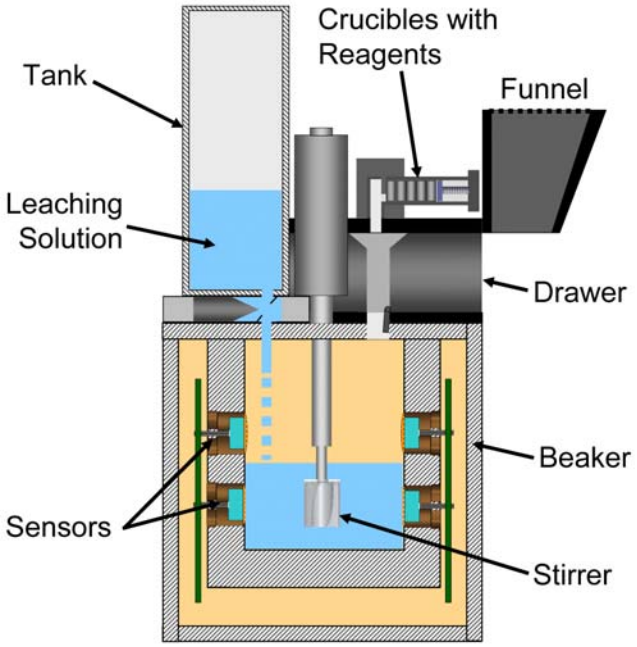

Figure 1. Schematic diagram of the WCL interior showing the relative configuration of the various components (not to scale).

suggested that past, and perhaps present, aqueous geochemistry at widely separated locations on Mars is consistent with an environment that is acidic and rich in sulfates [*Ming et al.*, 2008; *Hurowitz et al.*, 2006; *Tosca et al.*, 2005; *Tosca and McLennan* 2006]. The OMEGA imaging spectrometer on Mars Express has identified calcium-rich sulfates, probably gypsum, approximately 700 km north of the Phoenix landing site corresponding to a large area covered by dunes. Such observations suggest that water alteration has played a major role in the formation of the minerals in the area of the Phoenix site [*Langevin et al.*, 2005; *Bibring and Langevin*, 2008].

[3] There have been observations, models, and experiments, however, that have suggested an alkaline soil and carbonates. Simulations of the Viking gas exchange experiment using palagonite and Fe-rich montmorillonite exposed to the Viking nutrient solution, showed that to simulate the CO_2 gas changes, the soil/nutrient/solution mixture need to be at a pH between 7.4 and 8.7 [*Quinn and Orenberg*, 1993]. Evaporite sequence models have also suggested an early deposition of carbonates [*Catling*, 1999; *King et al.*, 2004].

[4] This paper details the initial findings from the aqueous chemistry experiments performed with the four WCLs at the Phoenix landing site. During the 152 sol mission, the robotic arm delivered soil samples to all four of the cells. Three of the soil samples were successfully transferred by the cell drawers to their respective beakers and analyzed. The fourth WCL cell showed no clear indication that soil had been mixed with the water in the beaker. Each WCL returned seven types of science data over one or more sols of analysis. The data types included (1) ISE potentials, (2) solution electrical conductivity, (3) pressure, (4) temperature, (5) redox potential, (6) voltammetry, and (7) chronopotentiometry. This paper presents an overview of the WCL operations throughout the mission and details the results for the ion selective electrodes (ISE) and electrical conductivity obtained on the sol when samples were first introduced to each cell.

2. Instrument Description

[5] Detailed descriptions of the WCL cell, its sensors, components, analytical protocol, and prelaunch characterizations, have been previously published [*Kounaves et al.*, 2009a; 2003] and are only briefly summarized here. Figure 1 shows a schematic diagram of the WCL. All four WCLs (designated as cells 0–3) were identical. Each one consisted of (1) an upper actuator assembly with a drawer for adding $\sim$1 cm^3 of soil, 25 mL of "leaching solution" (deionized water with 1×10^{-5} M of each detectable ion except for 5×10^{-5} M Cl^- and 1×10^{-3} M Li^+ and NO_3^-), five crucibles with reagents, and a stirrer, and (2) a lower beaker lined with an array of sensors. The sensors included six membrane-based ion selective electrodes (ISE) for measuring Ca^{2+}, Mg^{2+}, K^+, Na^+, and NH_4^+, one IrO_2 and two ISEs for pH, an ISE responsive primarily to ClO_4^-, a Ba^{2+} ISE for titrimetric determination of SO_4^{2-}, two Li^+ ISEs as references, three crystal pellet ISEs for Cl^-, Br^-, and I^-, an electrode for conductivity, a Pt and two Ag electrodes for chronopotentiometric (CP) determination of Cl^-, Br^-, and I^-, and a Au electrode for cyclic voltammetry (CV).

3. WCL Operations Overview

[6] The postlaunch operation of the WCLs can be divided into three phases: cruise checkouts, surface characterization, and surface science.

3.1. Cruise Phase Checkouts

[7] During the cruise phase of the mission the two WCL instrument checkouts consisted of monitoring pressure and temperature for 30 s in each of the WCLs. These tests showed that the temperature and pressure sensors, other than exhibiting somewhat higher levels of noise than expected, were functioning normally and provided calibration data for those sensors.

3.2. Surface Characterization Phase Tests

[8] After Phoenix landed, the WCLs were tested six times during the surface characterization phase of the mission to verify their operational functionality (Table 1). The first three "PT monitor" tests on sols 1 and 4 consisted of performing pressure and temperature measurements for 1.5 min in each of the WCLs at different times during the Martian sol. For each test, data was collected from three temperature sensors onboard each WCL located in the beaker wall, on the drawer, and on the water tank (Figure 1). The test results were used to characterize the thermal environment of the WCLs at the landing site, as well as assess the functionality of their pressure and temperature sensors.

[9] The characterization phase on sol 4 consisted of supplying power to the heaters and actuators of each WCL in succession while monitoring power, pressure, and temperature. The power data returned from the checkout

Table 1. Description of Characterization Phase WCL Activities[a]

Sol	Name	Description	Start Time (SCLK)	Start Time (LMST)
001	PT Monitor A	Pressure and temperature were monitored in	896302407	12:59:59
	PT Monitor B	each of the WCL cells for 1.5 min.	896311314	15:24:28
004	PT Monitor C	Pressure and temperature were monitored in each of the WCL cells for 1.5 min. The commanding sequence was executed twice in a row.	896562377	11:16:53
004	Copper Checkout	Heater and actuator circuitry were tested for each of the WCL cells.	896577345	15:19:40
005	Checkout A	Tested temperature control loop for tank and drawer, cycled drawer (burped), monitored ISEs, pressure, temperature, and conductivity in cell 0.	896651616	11:24:24
007	Checkout B	Tested temperature control loop for tank and drawer, cycled drawer (burped), monitored ISEs, pressure, temperature, and conductivity in cells 1, 2, and 3.	896834207	12:46:09

[a]WCL, Wet Chemistry Laboratories; SCLK, spacecraft clock time; LMST, local mean solar time.

verified proper electrical connectivity and power draw for all of the heaters and actuators on each of the WCLs. On sol 5, the "checkout A" activity tested the full functionality of several components and sensors on cell 0 (Beaker s/n 020). In order, this involved powering the tank heater for 5 min, powering the drawer heater for 5 min, opening and closing the sample drawer, and acquiring 1.5 min of ion selective electrode data (solution from the tank had not yet been added) and 1.5 min of conductivity data. Pressure and temperature were monitored throughout the entire test except when collecting conductivity data. The "checkout B" activities on sol 7 repeated those of checkout A in cells 1–3. Both checkout A and checkout B indicated normal operation of the sample drawers and the heaters. The signals from the tank, beaker, and drawer temperature sensors were as expected. There were some electronic offsets and noise due to powering heaters, but these were corrected during subsequent WCL science phase activities.

3.3. Surface Science Phase

[10] After the characterization phase, the WCLs were operated 21 times during the surface science phase of the mission to perform the wet chemical analyses of the soil samples as well as a number of procedural and diagnostic tests (Table 2). The core of WCL operations consisted of a 2 sol analysis of each acquired sample. The primary samples, designated as Rosy Red, Sorceress 1, Sorceress 2, and Golden Goose, were acquired from four locations by the robotic arm (RA) [*Arvidson et al.*, 2009; *Shaw et al.*, 2009]. Rosy Red was acquired on sol 25 from the surface of the Burn Alive trench and delivered on sol 30 to WCL cell 0. Sorceress 1, acquired on sol 35 from the Snow White trench, was a sublimation lag sample from the surface of the ice cemented soil at a depth of about 5 cm. It was delivered to WCL cell 1 on sol 41. Sorceress 2, acquired on sol 105 adjacent to Sorceress 1, was delivered to WCL cell 2 on sol 107. Golden Goose, the deepest sample from ~16 cm, was acquired on sol 95 from the Stone Soup trench and delivered on sol 96 to WCL cell 3. The Rosy Red, Sorceress 1, and Sorceress 2 samples were successfully transported by the WCL drawers into their respective cells (0, 1, and 2) and analyzed. The Golden Goose sample for cell 3 appeared to lodge in the delivery funnel, thus, cell 3 was run as a blank.

Table 2. Summary of the WCL Sample Delivery Activities for Each Sol

CELL 0, Beaker 020		CELL 1, Beaker 018		CELL 2, Beaker 022		CELL 3, Beaker 014	
Sol	Activity	Sol	Activity	Sol	Activity	Sol	Activity
030	First delivery: Rosy Red (see Table 3)	041	First delivery: Sorceress 1 (see Table 4)	107	First delivery: Sorceress 2 (see Table 5)	096	First Delivery: Golden Goose (see Table 6)
032	Beaker thaw	043	Acid and $BaCl_2$ crucibles added	116	Acid and first $BaCl_2$ crucible addition	102	Second delivery (Golden Goose 2)
034	Acid and $BaCl_2$ crucibles addition			127	Second $BaCl_2$ crucible addition	147	Sample push by robotic arm
066	Second delivery (Rosy Red 2)			131	Beaker thaw		
078	Thermal diagnostic run			134	Third $BaCl_2$ crucible and ORP diagnostic		
087	Open loop diagnostic run						
138	Third delivery (Rosy Red 3)						

Table 3. Sol 030 Rosy Red Delivery Events[a]

Event	Start Time (SCLK)	Start Time (LMST)	Duration (min:s)	Notes
		Tank Thaw		
Thaw LS in tank until set point reached	898863739	0926:36	40:11	Set Point = 2314DN (10°C), PT data
Temperature control at set point	898866150	1005:42	05:01	PT data collection
Dispense LS into beaker	898866468	1010:52	05:01	Stirrer on, PT data collection
		Calibration		
ISEs and conductivity data	898866770	1015:46	20:55	2x(ISEs/PT (∼9 min) and EC (∼1 min))
Voltammetry	898868025	1036:07	01:22	3 CP Ramps
Drawer commanded to open (burp)	898868112	1037:32	02:59	ISEs/PT continuous data collection
Drawer commanded to closed (burp)	898868292	1040:27	04:01	ISEs/PT continuous data collection
ISEs and conductivity data	898868533	1044:21	21:03	2x(ISEs/PT (∼9 min) and EC (∼1 min))
Voltammetry	898869796	1104:50	01:22	3 CP Ramps
Drawer commanded to open (burp)	898869883	1106:15	03:01	ISEs/PT continuous data collection
Drawer commanded to close (burp)	898870064	1109:11	04:01	ISEs/PT continuous data collection
Calibrant crucible release	898870317	1113:18	05:02	
ISEs and conductivity data	898870619	1118:12	10:32	ISEs/PT (∼9 min) and EC (∼1 min)
Voltammetry	898871252	1128:27	18:48	24 CV Scans, 6 CP Ramps, 9 CP Steps
ISEs and conductivity data	898872380	1146:45	10:31	ISEs/PT (∼9 min) and EC (∼1 min)
		Sample Delivery and Verification		
Drawer commanded to open	898873507	1205:02	03:01	ISEs/PT continuous data collection
Drawer commanded to close	898873872	1210:57	04:00	ISEs/PT continuous data collection
Conductivity data	898874118	1214:57	00:59	
Drawer commanded to open	898874252	1217:07	02:39	ISEs/PT continuous data collection
Drawer commanded to close	898874478	1220:47	04:02	ISEs/PT continuous data collection
Conductivity data	898874725	1224:48	01:01	
		Analysis		
ISEs and conductivity data	898874889	1227:28	20:45	2x(ISEs/PT (∼9 min) and EC (∼1 min))
Voltammetry	898876135	1247:39	27:15	36 CV Scans, 8 CP Rams, 16 CP Steps
ISEs and conductivity data	898877769	1314:11	31:29	3x(ISEs/PT (∼9 min) and EC (∼1 min))
Voltammetry	898879658	1344:49	27:12	36 CV Scans, 8 CP Rams, 16 CP Steps
ISEs and conductivity data	898881290	1411:17	31:32	3x(ISEs/PT (∼9 min) and EC (∼1 min))
Voltammetry	898883182	1441:58	27:17	36 CV Scans, 8 CP Rams, 16 CP Steps
ISEs and conductivity data	898884819	1508:32	135:03	13x(ISEs/PT (∼9 min) and EC (∼1 min))
Turn off WCL	898892922	1719:58	00:54	

[a]SCLK, spacecraft clock time; LMST, local mean solar time; LS, leaching solution; PT, pressure/temperature; CV, cyclic voltammetry; CP, chronopotentiometry; EC, electrical conductivity.

[11] Samples typically sat in the RA scoop for 1–3 sols, protected from direct sunlight whenever possible. During the sol the air temperatures varied between −32 and −80°C at the start of the mission, to between −45 and −98°C at the end. All soil samples appeared to be dry when delivered to the WCL. The soil in the scoop often appeared to be clumpy, but small clumps would disintegrate after sitting in the scoop for one sol.

[12] There was no direct method to ascertain the porosity of the soil, or to determine either the bulk or disturbed density of the soil, thus, based on Viking results we assumed a density of 1.0 g/cm^3. The physical properties of the soils are described in more detail elsewhere [*Arvidson et al.*, 2009; *Shaw et al.*, 2009; W. Goetz et al., Microscopic structure of soils at the Phoenix landing site, Mars: Classification and description of their optical and magnetic properties, submitted to *Journal of Geophysical Research*, 2009].

[13] The first of the 2 sol analysis (sol A) began with the thawing and dispensing the 25 mL of leaching solution into the analysis beaker. After equilibration of sensors in the leaching solution, a second calibration point was obtained by adding a crucible of known salt content to the beaker that increased concentrations to between 3.4×10^{-5} M to 2×10^{-4} M depending on the ion [*Kounaves et al.*, 2009a]. After calibration, the soil sample that had been acquired by the RA was delivered to the WCL sample drawer. The drawer, which holds 1 cm^3 of soil, was imaged with the RAC to determine the volume of the soil and confirm delivery. Images of Rosy Red and Sorceress 2 after delivery showed the drawer completely full. The image for Sorceress 1 showed the drawer approximately 70–75% full. The filled drawer was then retracted and the soil dispensed into the leaching solution and monitored for the remaining portion of the sol. Throughout the sol, data were continuously collected from the ISEs, pressure, and temperature sensors, with short pauses to acquire electrical conductivity measurements and voltammetry scans. The solution/soil mixture was allowed to freeze at the end of the sol. The operational events for the sol A analyses on sols 30, 41, 96, and 107 (cells 0, 1, 3, and 2, respectively) are compiled in Tables 3–6.

[14] The second sol of analysis (sol B) began by thawing the solution in the beaker for a predetermined time (Table 2). Following the thaw, the crucible containing 0.004 g of 2-nitrobenzoic acid was added with the purpose of determining the solution's pH buffering capacity. After the acid addition experiment, titration of possible sulfate in solution was performed by sequential addition of one or more crucibles containing ∼0.11 g of $BaCl_2$. For Sorceress 2 the second and third $BaCl_2$ crucibles were postponed to sols 127 and 134. As before, sensors were continually monitored through the duration of the sol. Sol B analyses occurred on sol 34 for cell 0, sol 43 for cell 1, and sols 116, 127, 131, and 134 for cell

Table 4. Sol 041 Sorceress 1 Delivery Events[a]

Event	Start Time (SCLK)	Start Time (LMST)	Duration (min:s)	Notes
		Tank Thaw		
Thaw LS in the tank until set point	899840638	0932:35	43:12	Set Point = 2521DN (16°C), PT data
Temperature control at set point	899843231	1014:38	05:01	PT data collection
Dispense of solution into beaker	899843548	1019:48	05:01	Stirrer on, PT data collection
		Calibration		
ISEs and conductivity data	899843851	1024:41	20:15	2x(ISEs/PT (∼9 min) and EC (∼1 min))
Voltammetry	899845066	1044:24	01:20	3 CP Ramps
Drawer commanded to open (burp)	899845150	1045:46	03:27	ISEs/PT continuous data collection
Drawer commanded to close (burp)	899845358	1049:08	04:02	ISEs/PT continuous data collection
ISEs and conductivity data	899845599.	1053:03	20:15	2x(ISEs/PT (∼9 min) and EC (∼1 min))
Voltammetry	899846814.	1112:46	01:20	3 CP Ramps
Drawer commanded to open (burp)	899846899	1114:08	03:17	ISEs/PT continuous data collection
Drawer commanded to close (burp)	899847096	1117:20	04:02	ISEs/PT continuous data collection
Calibrant crucible release	899847350	1121:27	05:04	
ISEs and conductivity data	899847654	1126:23	10:09	ISEs/PT (∼9 min) and EC (∼1 min)
Voltammetry	899848264	1136:17	18:24	24 CV Scans, 6 CP Ramps, 9 CP Steps
ISEs and conductivity data	899849368	1154:11	10:05	ISEs/PT (∼9 min) and EC (∼1 min)
		Sample Delivery and Verification		
Drawer commanded to open	899850468	1212:02	07:20	ISEs/PT continuous data collection
Drawer commanded to close	899850909	1219:10	04:02	ISEs/PT continuous data collection
Conductivity data	899851156	1223:11	01:07	
Drawer commanded to open	899851297	1225:28	03:53	ISEs/PT continuous data collection
Drawer commanded to close	899851772	1229:15	04:02	ISEs/PT continuous data collection
Conductivity data	899851778	1233:16	01:07	
		Analysis		
ISEs and conductivity data	899851948	1236:02	20:10	2x(ISEs/PT (∼9 min) and EC (∼1 min))
Voltammetry	899853157	1255:39	26:46	36 CV Scans, 8 CP Rams, 16 CP Steps
ISEs and conductivity data	899854763	1321:42	30:43	3x(ISEs/PT (∼9 min) and EC (∼1 min))
Voltammetry	899856606	1351:36	26:51	36 CV Scans, 8 CP Rams, 16 CP Steps
ISEs and conductivity data	899858217	1417:43	30:24	3x(ISEs/PT (∼9 min) and EC (∼1 min))
Voltammetry	899860042	1447:19	26:46	36 CV Scans, 8 CP Rams, 16 CP Steps
ISEs and conductivity data	899861648	1513:22	130:28	13x(ISEs/PT (∼9 min) and EC (∼1 min))
Turn off WCL	899869475	1720:20	0:54	

[a]SCLK, spacecraft clock time; LMST, local mean solar time; LS, leaching solution; PT, pressure/temperature; CV, cyclic voltammetry; CP, chronopotentiometry; EC, electrical conductivity.

2. The sol B analysis was never performed with cell 3 due to lack of sample and the end of the mission.

[15] The exact timing of the measurements and the steps described above for both sol A and sol B analyses varied between experiments, and additional analyses other than the typical sol A and sol B experiments included secondary sample additions and diagnostic tests for troubleshooting (Table 2). Analyses beyond sol A will be describe in a subsequent publication.

[16] Based on preflight sensor characterization [*Kounaves et al.*, 2009a], and sensor behavior during surface operations, there was no indication that any of the sensors had been ''poisoned'' by any of the species present in any of the Martian soil samples analyzed.

4. Data Processing and Analysis

[17] The data returned for each WCL analysis included voltage readings from the ISEs, pressure, redox, and temperature sensors, and both voltage and current readings from the conductivity sensors and voltammetry (CV/CP) measurements. All voltage and current data were returned in the form of digital numbers (DN). They were converted to voltage and current values using parameters determined from preflight calibration of the MECA analog electronics board. Preflight calibration parameters were also used for the conversion of electrical conductivity (EC) sensor current and voltage DNs to solution resistivity, proportional to the inverse of conductance. For the pressure and temperature data, DN to degrees Celsius and DN to mbar conversions were obtained using a combination of preflight, cruise, and characterization phase measurements. Second-level processing of the ISE voltage data and the conductivity data are described in the following sections.

4.1. Ion Selective Electrode Signal Processing

[18] The voltage measured by the ISEs relative to the platinum oxidation reduction potential electrode (ORP) unexpectedly exhibited varying levels of systematic fluctuations. These were found to result from periodic temperature measurements that, due to a software error, caused the ORP to switch between a 650 mV source and ground. The largest fluctuations were eliminated by discarding every ISE data point that directly preceded a temperature measurement. ISE potentials were subsequently referenced to either of two Li^+ ISEs, whose potential was stabilized by 10^{-3} M $LiNO_3$ in solution. As an example, Figure 2 shows the results of signal processing for the Na^+ ISE (Sorceress 2, sol 107) which was adversely affected by the ORP fluctuations during temperature measurements.

[19] Since the ISE sensors were read consecutively, the rapid fluctuation of the ORP potential sometimes caused deviations between the two Li^+ ISEs. These were resolved by selecting as reference for each ISE signal the Li^+ ISE that most strongly correlated with its behavior (i.e., minimized drift). Additional data points were removed when events

Table 5. Sol 107 Sorceress 2 Delivery Events[a]

Event	Start Time (SCLK)	Start Time (LMST)	Duration (min:s)	Notes
		Tank Thaw		
Thaw LS in tank until set point	905698777	0915:43	50:15	Set Point = 2133DN (15°C), PT data
Temperature control at set point	905701792	1004:38	04:01	PT data collection
Dispense of solution into beaker	905702050	1008:49	05:01	PT data collection
		Calibration		
Set temperature, wait for set point	905702369	1014:00	15:03	Stirrer on, ISEs/PT data collection
ISEs and conductivity data	905703273	1028:39	30:36	3x(ISEs/PT (∼9 min) and EC (∼1 min))
Voltammetry	905705110	1058:27	02:01	3 CP Ramps
ISEs and conductivity data	905705230	1100:24	30:43	3x(ISEs/PT (∼9 min) and EC (∼1 min))
Voltammetry	905707073	1130:18	01:59	3 CP Ramps
Drawer commanded to open (burp)	905707200	1132:21	03:25	ISEs/PT continuous data collection
Drawer commanded to close (burp)	905707406	1135:42	04:01	ISEs/PT continuous data collection
15 min ISEs/PT data collection	905707647	1139:36	15:06	ISEs/PT continuous data collection
Drawer commanded to open (burp)	905708553	1154:18	03:25	ISEs/PT continuous data collection
Drawer commanded to close (burp)	905708758	1157:38	04:00	ISEs/PT continuous data collection
Calibrant crucible release	905709012	1201:45	05:00	
ISEs and conductivity data	905709312	1206:37	40:53	4x(ISEs/PT (∼9 min) and EC (∼1 min))
Voltammetry	905711765	1246:24	49:47	84 CV's, 3 DO Scans, 6 CP Ramps, 9 CP Steps, 3 ORP Cleaning Scans
ISEs and conductivity data	905714753	1334:52	41:04	4x(ISEs/PT (∼9 min) and EC (∼1 min))
		Sample Delivery and Verification		
Drawer commanded to open	905720225	1503:38	03:26	ISEs/PT continuous data collection
Drawer commanded to close	905720959	1515:32	04:01	ISEs/PT continuous data collection
Conductivity data	905721203	1519:30	01:09	
Drawer commanded to open	905721545	15:25:03	03:23	ISEs/PT continuous data collection
Drawer commanded to close	905722014	1532:39	04:00	ISEs/PT continuous data collection
Conductivity data	905722260	1536:38	01:07	
		Analysis		
ISEs and conductivity data	905722599	1542:08	51:07	5x(ISEs/PT (∼9 min) and EC (∼1 min))
Voltammetry	905725666	1631:54	34:02	36 CV Scans, 3 DO Scans, 8 CP Rams, 16 CP Steps, 3 ORP Cleaning Scans
ISEs and conductivity data	905727709	1705:01	61:05	6x(ISEs/PT (∼9 min) and EC (∼1 min))
Voltammetry	905731399	1804:53	32:54	36 CV Scans, 3 DO Scans, 8 CP Rams, 16 CP Steps, 3 ORP Cleaning Scans
ISEs and conductivity data	905733373	1836:54	61:20	6x(ISEs/PT (∼9 min) and EC (∼1 min))
Voltammetry	905737053	1936:35	33:16	36 CV Scans, 3 DO Scans, 8 CP Rams, 16 CP Steps, 3 ORP Cleaning Scans
ISEs and conductivity data	905739065	2009:14	10:19	ISEs/PT (∼9 min) and EC (∼1 min)
Turn off WCL	905739739	2020:10	00:10	WCL closed out by Science Master

[a]SCLK, spacecraft clock time; LMST, local mean solar time; LS, leaching solution; PT, pressure/temperature; CV, cyclic voltammetry; CP, chronopotentiometry; EC, electrical conductivity.

such as the drawer opening and closing caused transient temperature excursions. Random noise was then reduced by signal averaging, Fourier filtering, and removal of obvious outliers, presumably due to electronic transients. The resulting processed signals for the sol A analysis for samples delivered on sols 30, 41, 107, and 96, are shown in Figures 3, 4, 5, and 6, respectively.

4.2. Conversion of ISE Potentials to Ion Activity and Concentration

[20] The conversion of ISE voltages to ionic activities and concentrations was made using a combination of preflight calibrations [*Kounaves et al.*, 2009a], surface calibrations, and post flight laboratory calibrations and experiments. To convert from the measured ISE potential to ionic (activity) and [concentration] in the solution/soil mixture, requires use of a calibration slope and intercept. For determining the activity of Na^+, K^+, Mg^{2+}, NH_4^+ and Cl^-, we used the slope obtained by averaging four preflight calibrations that were corrected for the temperature on Mars, the calibrant ISE potential measured on Mars, and a calculated intercept. Since the ISEs are Nernstian in their response [*Kounaves et al.*, 2009a], the slope on Mars (S_M) is given by

$$S_M = S_E(T_M/T_E) \quad (1)$$

where S_E is the preflight slope on Earth in mV/decade activity, and T_M and T_E are the temperature on Mars and Earth in Kelvin. The calibrant intercept (E_I) was determined by selecting a specific time interval before sample addition (Figures 3–6 and Table 7), at a relatively stable calibrant potential (E_C) averaged over that interval, and substituting into the Nernst equation

$$E_I = E_C - S_M \log(a_C) \quad (2)$$

where a_C is the known activity of the added calibrant ion. For the Rosy Red, Sorceress 2 and Golden Goose samples,

Table 6. Sol 096 Golden Goose Delivery Events[a]

Event	Start Time (SCLK)	Start Time (LMST)	Duration (min:s)	Notes
		Tank Thaw		
Thaw LS in the tank until set point	904722247	0915:44	48:13	Set Point = 2030DN (15°C), PT data
Temperature control at set point	904725140	1002:39	05:01	PT data collection
Dispense of solution into beaker	904725459	1007:49	05:01	PT data collection
		Calibration		
Set temperature control and wait for set point	904725779	1013:01	10:02	Stirring initiated, ISEs/PT data collection
ISEs and Conductivity Data	904726383	1022:48	17:24	2x(ISEs/PT (∼8 min) and EC (∼1 min))
Voltammetry	904727427	1039:45	01:50	3 CP Ramps
ISEs and Conductivity Data	904727537	1041:32	17:23	2x(ISEs/PT (∼8 min) and EC (∼1 min))
Voltammetry	904728580	1058:27	01:51	3 CP Ramps
Drawer commanded to open (“Burp”)	904728691	1100:15	03:25	ISEs/PT continuous data collection
Drawer commanded to close (“Burp”)	904728896	1103:35	04:03	ISEs/PT continuous data collection
15 min ISEs/PT data collection	904729139	1107:31	15:00	ISEs/PT continuous data collection
Drawer commanded to open (“Burp”)	904730045	1122:13	03:26	ISEs/PT continuous data collection
Drawer commanded to close (“Burp”)	904730251	1125:34	04:03	ISEs/PT continuous data collection
Calibrant Crucible Release	904730507	1129:42	05:00	
ISEs and Conductivity Data	904730807	1134:34	08:42	1x(ISEs/PT (∼8 min) and EC (∼1 min))
Voltammetry	904731328	1143:02	48:11	90 CV Scans, 3 DO Scans, 6 CP Ramps, 9 CP Steps, 3 ORP Cleaning Scans
ISEs and Conductivity Data	904734219	1229:55	17:13	2x(ISEs/PT (∼8 min) and EC (∼1 min))
		Sample Delivery and Verification		
Drawer commanded to open	904737828	1328:28	07:50	ISEs/PT continuous data collection
Drawer commanded to close	904738686	1342:23	02:51	ISEs/PT continuous data collection
Conductivity Data	904738863	1345:15	01:08	
Drawer commanded to open	904739013	1347:41	07:50	ISEs/PT continuous data collection
Drawer commanded to close	904739559	1356:32	04:31	ISEs/PT continuous data collection
Conductivity Data	904739836	1401:02	01:05	
		Analysis		
ISEs and Conductivity Data	904739986	1403:28	17:08	2x(ISEs/PT (∼8 min) and EC (∼1 min))
Voltammetry	904741015	1420:09	31:40	36 CV Scans, 3 DO Scans, 8 CP Rams, 16 CP Steps, 6 ORP Cleaning Scans
ISEs and Conductivity Data	904742915	1450:58	25:51	3x(ISEs/PT (∼8 min) and EC (∼1 min))
Voltammetry	904744465	1516:07	32:31	36 CV Scans, 3 DO Scans, 8 CP Rams, 16 CP Steps, 6 ORP Cleaning Scans
ISEs and Conductivity Data	904746416	1547:46	25:26	3x(ISEs/PT (∼8 min) and EC (∼1 min))
Voltammetry	904747962	1612:51	31:22	36 CV Scans, 3 DO Scans, 8 CP Rams, 16 CP Steps, 6 ORP Cleaning Scans
ISEs and Conductivity Data	904749843	1643:22	25:50	3x(ISEs/PT (∼8 min) and EC (∼1 min))
Voltammetry	904751394	1708:31	31:44	36 CV Scans, 3 DO Scans, 8 CP Rams, 16 CP Steps, 6 ORP Cleaning Scans
ISEs and Conductivity Data	904753299	1739:24	08:32	ISEs/PT (∼8 min) and EC (∼1 min)
Turn Off WCL	904753810	1747:42	00:53	

[a]SCLK, spacecraft clock time; LMST, local mean solar time; LS, leaching solution; PT, pressure/temperature; CV, cyclic voltammetry; CP, chronopotentiometry; EC, electrical conductivity.

we assumed that the calibrant crucibles had fully delivered their contents. This is a reasonable assumption since the ΔE for the addition was as predicted from the preflight calibrations. For Sorceress 1, the crucible was deployed but the calibrant salts did not appear to dissolve before the sample was added.

[21] Once proper calibration slopes and intercepts had been defined for each sensor, a second time interval shortly after sample addition was selected for determining activity (Figures 3–6 or Table 7). The log (activity) of the sample ions (a_S) were calculated by using

$$\log(a_S) = (E_S - E_I)/S_M \tag{3}$$

where E_S is the averaged potential over the selected sample time interval, S_M is the temperature-corrected slope, and E_I is the calculated intercept from equation (2). After the activity of each ion in solution was calculated, it was converted to concentration (C) using $C = a/\gamma$, where γ is the activity coefficient. The activity coefficient was calculated using the Debye-Hückel equation

$$\log\gamma = \frac{-0.51z^2\sqrt{\mu}}{1 + (\alpha\sqrt{\mu}/305)} \tag{4}$$

where z is the ionic charge, α is the radius of the hydrated ion, and μ is the total ionic strength in mol/L. Ionic strength can determined using the solution’s electrical conductivity (EC) and an empirically derived constant [*Griffin and Jurinak*, 1973]. For Sorceress 1, Sorceress 2, and Golden Goose, the constant was determined experimentally [*Kounaves et al.*, 2009a] for the ions known to be in the sample solution and μ can then be calculated from the relationship

$$\mu = 0.0135(\pm 0.0002)\mathrm{EC} \tag{5}$$

where EC is in mS/cm (at 25°C) and measured as close as possible to the same time interval selected for the sample analysis.

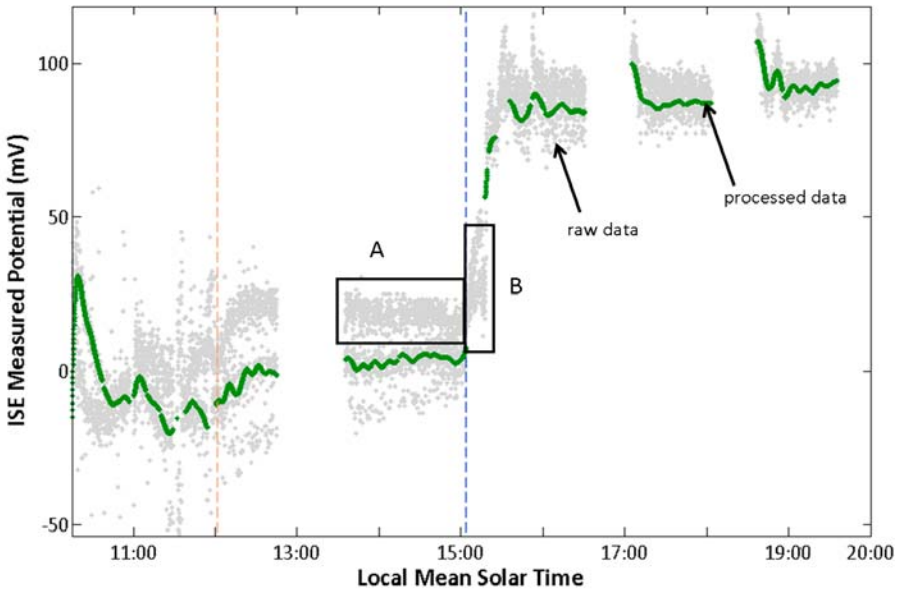

Figure 2. Processing of a particularly poor signal for Sorceress 2 on sol 107. Points in region A exemplify points adversely affected by the ORP fluctuations that resulted from temperature measurements. They were easily identified by the bimodal distribution and were removed. The points in box B were removed since they were adversely affected by large thermal and ORP fluctuations due to drawer open and close events. The remaining data were filtered, resulting in the final processed signal.

[22] Since there was no conductivity data obtained for Rosy Red (due to a software fault) we calculated μ by assuming, as a first-order approximation, that $C \approx a$. The ionic strength was then obtained from

$$\mu = \frac{1}{2}\sum_i c_i z_i^2 \tag{6}$$

where C_i is the concentration of the ith ion and z_i is its charge. This assumption is valid since C is conservatively within 25% of a at the activities measured in cell 0 for divalent ions and within 10% for monovalent ions. Propagation of these conservative errors in C for each *unknown* ion via equations (6) and (4) yields only a few percent error in the final calculated activity coefficients and concentration values, which is insignificant compared to the larger concentration errors indicated in Table 7. The ionic

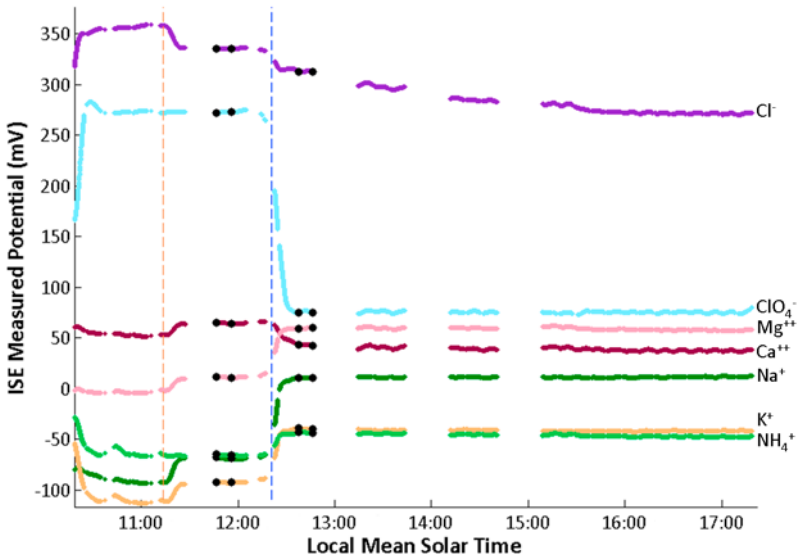

Figure 3. Sensors response for the analysis of the Rosy Red sample on sol 30 in cell 0. The two vertical lines indicate the addition of the calibrant crucible and the soil sample. The x axis indicates the sol and local mean solar time. Cations and anions show a positive and negative potential change, respectively, for an increase in concentration.

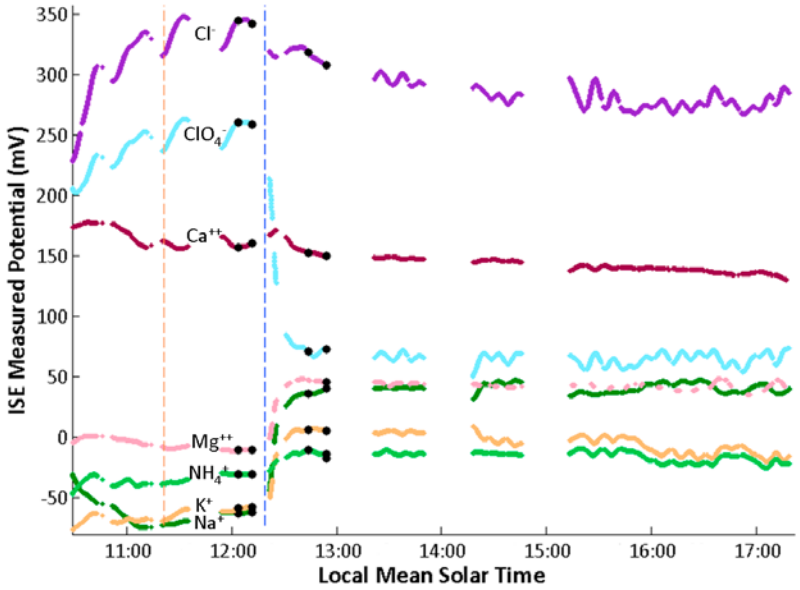

Figure 4. Sensors response for the analysis of the Sorceress 1 sample on sol 41 in cell 1. The two vertical lines indicate the addition of the calibrant crucible and the soil sample. The *x* axis indicates the sol and local mean solar time. Cations and anions show a positive and negative potential change, respectively, for an increase in concentration.

strength was then used in equation (4) to calculate the activity coefficients necessary for converting activities to concentrations.

[23] Table 7 shows the calibration, data analysis parameters, and results for the sol A analysis of the four soil samples. The major uncertainties in the concentration values arise primarily from, the standard deviations in Nernstian slopes of the four preflight calibrations, ISE potential and temperature measurement instabilities within the time intervals selected for calibration and sample analysis, and uncertainties in the electrical conductivity values. For example, the Nernstian slope of the potassium ISE for cell 0 (sol 30) had an uncertainty of 3.4 mV as determined from preflight calibration, and the solution temperature measurement was uncertain to 0.9 and 0.7°C at the times when the calibration and sample potentials were selected, respectively. Also, the selected potentials of the potassium ISE calibration and the sample measurement had uncertainties of

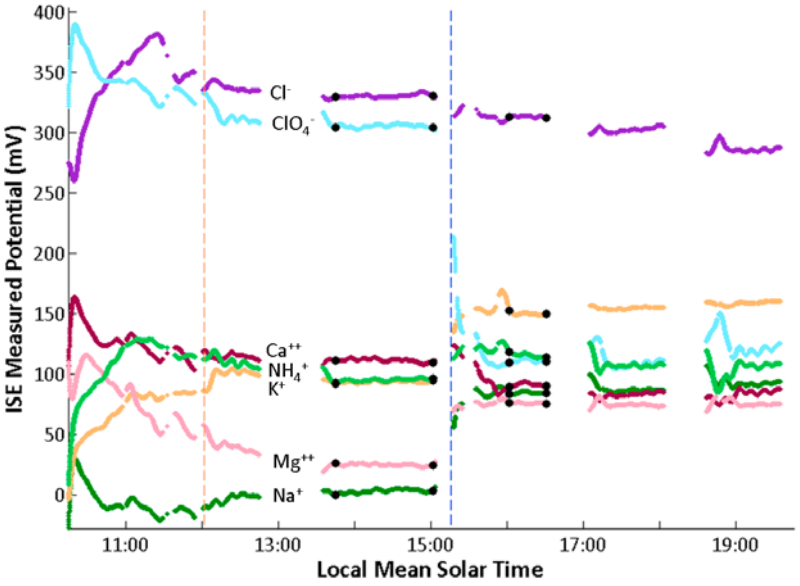

Figure 5. Sensors response for the analysis of the Sorcress 2 sample on sol 107 in cell 2. The two vertical lines indicate the addition of the calibrant crucible and the soil sample. The *x* axis indicates the sol and local mean solar time. Cations and anions show a positive and negative potential change, respectively, for an increase in concentration.

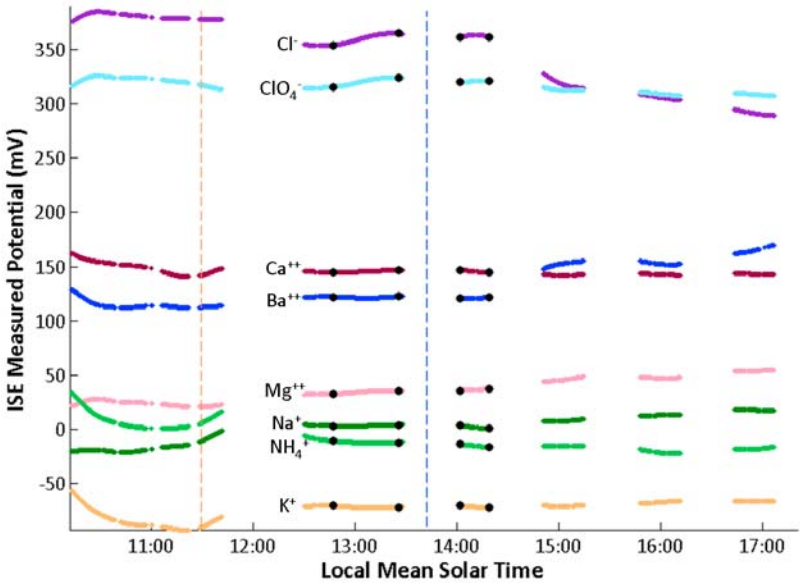

Figure 6. Sensors response for the attempted analysis of the Golden Goose sample on sol 96 in cell 3. The two vertical lines indicate the addition of the calibrant crucible and the soil sample. The *x* axis indicates the sol and local mean solar time. Cations and anions show a positive and negative potential change, respectively, for an increase in concentration.

0.6 mV and 0.8 mV, respectively. Each of these errors, along with the error in conductivity (as described in section 4.4), was propagated through the calculations converting ISE potentials to concentrations using standard error propagation techniques. All other errors, including the assumption that $C \approx a$, were negligible.

[24] The NH_4^+ ISE was treated differently for the activity calculation since it can also respond to K^+. Accordingly, the activity of NH_4^+ in solution, a_{NH4}, was replace by (a_{NH4+} + $K^*a_{K^+}$) in equation (2) above, where K^* is the selectivity coefficient for K^+ on the NH_4^+ ISE and is equal to 0.15 for these electrodes. Calibrations and calculations for the ClO_4^- and Ca^{2+} were unique and are handled later in further detail.

[25] For anions, an increase in concentration corresponds to a negative change in potential. As can be seen in Figures 3–6, the Cl^- ISE potential appears to consistently decrease by several 100 mV after the addition of the sample. This observation was initially interpreted as perhaps resulting from either, the sample leaching chloride, or sensor drift. However, due to the inability to deliver a sample into the beaker of cell 3 on sol 96, this cell became a de facto "blank" run (Figure 6). During this blank run, it is clearly evident that the chloride and barium ISEs measure a continual increase of Ba^{2+} and Cl^- ions in the solution after the drawer was opened/closed (burped) for the sample. There is no evidence that any $BaCl_2$ was released before the sampling phase of the analysis. Since no detectable amount of soil was added to this cell, the increase is most consistent with accidental addition of Ba^{2+} and Cl^- from one of the three crucibles containing 0.1 g of $BaCl_2$. The same behavior is also exhibited in the other three cells after the soil is added.

[26] We suspect that a portion of the $BaCl_2$ was dislodged from the crucible and contaminated the upper part of the actuator assembly. After the drawer activations for sampling, enough moisture had condensed that it started to flow and/or drip into the beaker, bringing with it the $BaCl_2$ that had contaminated the upper chamber. The drips or flow occurred at intervals such that at some points a step response is seen while at others a gradual decrease is observed. Quantification of the Ba^{2+} and Cl^- shows that throughout the sol, there is twice the molar amount of Cl^- being added to the solution as Ba^{2+}, as would be expected for the addition of $BaCl_2$ from the crucible. This unintentional addition of Ba^{2+} may potentially affect the determination of the SO_4^{2-} and is currently under study.

4.3. Calibration and Determination of Perchlorate (ClO_4^-)

[27] Upon the addition of soil to the WCL beakers during surface operations, a 3 order-of-magnitude signal increase in the response of the Hofmeister ISE was observed (labeled ClO_4^- in Figures 3–5). This particular ISE responds to a large number of anionic species with the selectivity dictated by the Hofmeister series; $ClO_4^- > I^- > SCN^- > ClO_3^- > CN^- > Br^- > S_2O_8 = > BO_3^{3-} > NO_3^- > HS^- > HCO_3^- > Cl^-$. Several of these were tested in the laboratory by adding 3–6 mM of the ion to a WCL test bed cell and observing the response of all the sensors. Those tested included; SCN^-, ClO_3^-, CN^-, Br^-, BO_3^{3-}, and S_2O_8 = . The majority were eliminated as possible interferents due to (1) the absence of their detection on the halide ISEs on Mars, (2) their effects on the Ca^{2+}/Mg^{2+} ISEs, or (3) that it would require an amount of the ionic species equal to several times the mass of the sample delivered to give an appropriate response in the Hofmeister ISE. It was subsequently determined that of the plausible ions considered, the only one that gave a similar response in conjunction with the observed effects on the Ca^{2+} ISE was ClO_4^-. This of course does not insure that there is not some chemical species present in the Martian

Table 7. Calibration, Data Analysis Parameters, Error, and Results for All Samples and Cells

ISE	Ref	Calibrant Start Time (LMST)	Calibrant End Time (LMST)	Potential (mV)	Temp. (°C)	Calibration slope @T	Intercept (mV)	Sample Start Time (LMST)	Sample End Time (LMST)
Sol-30 Rosy Red Cell 0 FU#020 Sample Addition									
Na^+	Li_B	1146:46	1155:44	$-69.0^{+1.0}_{-0.4}$	$5.6^{+0.5}_{-0.4}$	$50.3^{+1.0}_{-1.0}$	$156.8^{+5.5}_{-4.9}$	1237:29	1246:26
K^+	Li_B	1146:46	1155:44	$-92.8^{+0.4}_{-0.2}$	$5.6^{+0.5}_{-0.4}$	$54.8^{+1.7}_{-1.7}$	$153.4^{+8.0}_{-7.8}$	1237:29	1246:26
Ca^{2+}	Li_B	1146:46	1155:44	$50.5^{+0.8}_{-0.5}$	$5.6^{+0.5}_{-0.4}$	$27.1^{+0.8}_{-0.8}$	$171.0^{+4.3}_{-4.1}$	1237:29	1246:26
Mg^{2+}	Li_B	1146:46	1155:44	$11.1^{+0.3}_{-0.2}$	$5.6^{+0.5}_{-0.4}$	$26.7^{+0.6}_{-0.6}$	$131.9^{+3.2}_{-3.1}$	1237:29	1246:26
Cl^-	Li_B	1146:46	1155:44	$335.3^{+0.2}_{-0.3}$	$5.6^{+0.5}_{-0.4}$	$-51.9^{+0.5}_{-0.5}$	$141.9^{+2.2}_{-2.3}$	1237:29	1246:26
ClO_4^-	Li_A	1146:46	1155:44	$272.7^{+0.4}_{-1.1}$	$5.6^{+0.5}_{-0.4}$	$-58.6^{+1.0}_{-1.1}$	$-78.8^{+6.8}_{-7.6}$	1237:29	1246:26
NH_4^+	Li_B	1146:46	1155:44	$-65.8^{+1.0}_{-0.3}$	$5.6^{+0.5}_{-0.4}$	$56.6^{+1.0}_{-1.0}$	$188.5^{+5.3}_{-4.6}$	1237:29	1246:26
Sol-41 Sorceress-1 Cell 1 FU#018 Sample Addition									
Na^+	Li_A	1204:01	1211:24	$-62.3^{+0.6}_{-0.5}$	$5.6^{+1.1}_{-0.7}$	$49.9^{+0.8}_{-0.7}$	$188.2^{+4.4}_{-4.0}$	1243:37	1254:18
K^+	Li_A	1204:01	1211:24	$-58.1^{+0.7}_{-0.8}$	$5.6^{+1.1}_{-0.7}$	$55.0^{+2.1}_{-2.0}$	$217.8^{+11.1}_{-10.8}$	1243:37	1254:18
Ca^{2+}	Li_A	1204:01	1211:24	$144.6^{+2.8}_{-1.3}$	$5.6^{+1.1}_{-0.7}$	$27.1^{+0.7}_{-0.7}$	$281.5^{+6.5}_{-4.7}$	1243:37	1254:18
Mg^{2+}	Li_B	1204:01	1211:24	$-10.5^{+0.7}_{-0.2}$	$5.6^{+1.1}_{-0.7}$	$25.9^{+0.8}_{-0.7}$	$120.7^{+4.1}_{-3.9}$	1243:37	1254:18
Cl^-	Li_B	1204:01	1211:24	$345.1^{+0.6}_{-2.6}$	$5.6^{+1.1}_{-0.7}$	$-51.4^{+0.5}_{-0.5}$	$122.9^{+2.6}_{-4.9}$	1243:37	1254:18
ClO_4^-	Li_B	1204:01	1211:24	$260.6^{+0.4}_{-1.6}$	$5.6^{+1.1}_{-0.7}$	$-58.5^{+0.9}_{-1.0}$	$-90.7^{+5.8}_{-7.5}$	1243:37	1254:18
NH_4^+	Li_A	1204:01	1211:24	$-30.4^{+0.3}_{-0.2}$	$5.6^{+1.1}_{-0.7}$	$56.1^{+1.4}_{-1.4}$	$251.1^{+7.5}_{-7.1}$	1243:37	1254:18
Sol-107 Sorceress-2 Cell 2 FU#022 Sample Addition									
Na^+	Li_A	1344:53	1501:13	$3.6^{+2.1}_{-3.0}$	$10.2^{+0.4}_{-0.4}$	$51.3^{+1.1}_{-1.1}$	$234.0^{+6.9}_{-7.8}$	1602:01	1630:34
K^+	Li_A	1344:53	1501:13	$93.9^{+2.2}_{-1.2}$	$10.2^{+0.4}_{-0.4}$	$55.5^{+1.3}_{-1.3}$	$343.3^{+7.9}_{-6.9}$	1602:01	1630:34
Ca^{2+}	Li_A	1344:53	1501:13	$97.5^{+2.4}_{-3.2}$	$10.2^{+0.4}_{-0.4}$	$27.8^{+0.3}_{-0.3}$	$221.3^{+3.8}_{-4.6}$	1602:01	1630:34
Mg^{2+}	Li_B	1344:53	1501:13	$25.3^{+1.5}_{-1.9}$	$10.2^{+0.4}_{-0.4}$	$27.4^{+0.6}_{-0.6}$	$149.3^{+4.0}_{-4.4}$	1602:01	1630:34
Cl^-	Li_B	1344:53	1501:13	$330.9^{+3.7}_{-1.6}$	$10.2^{+0.4}_{-0.4}$	$-52.0^{+0.7}_{-0.7}$	$137.0^{+5.1}_{-3.1}$	1602:01	1630:34
ClO_4^-	Li_A	1344:53	1501:13	$305.9^{+2.0}_{-2.9}$	$10.2^{+0.4}_{-0.4}$	$-59.5^{+0.3}_{-0.2}$	$-51.3^{+6.4}_{-7.4}$	1602:01	1630:34
NH_4^+	Li_A	1344:53	1501:13	$95.7^{+2.3}_{-3.1}$	$10.2^{+0.4}_{-0.4}$	$57.1^{+0.9}_{-0.8}$	$352.0^{+6.1}_{-6.9}$	1602:01	1630:34

ISE	Potential (mV)	Temp. (°C)	Calibration Slope @T	Activity (M)	Ionic Strength (M)	Activity Coefficient	Total Solution Concentration(M)
Sol-30 Rosy Red Cell 0 FU#020 Sample Addition							
Na^+	$10.4^{+0.3}_{-0.2}$	$8.4^{+0.4}_{-0.3}$	$50.8^{+1.0}_{-1.0}$	1.3E-03$^{+5.6E-04}_{-4.3E-04}$	8.4E-03$^{+4.2E-03}_{-6.7E-03}$	$0.91^{+0.03}_{-0.02}$	1.4E-03$^{+6.5E-04}_{-4.8E-04}$
K^+	$-39.9^{+0.5}_{-0.3}$	$8.4^{+0.4}_{-0.3}$	$55.4^{+1.7}_{-1.7}$	3.2E-04$^{+2.5E-04}_{-1.5E-04}$	8.4E-03$^{+4.2E-03}_{-6.7E-03}$	$0.91^{+0.03}_{-0.02}$	3.6E-04$^{+2.9E-04}_{-1.7E-04}$
Ca^{2+}	$77.6^{+3.0}_{-3.8}$	$8.4^{+0.4}_{-0.3}$	$27.3^{+0.8}_{-0.8}$	3.8E-04$^{+4.6E-04}_{-2.3E-04}$	8.4E-03$^{+4.2E-03}_{-6.7E-03}$	$0.69^{+0.09}_{-0.05}$	5.5E-04$^{+7.5E-04}_{-3.4E-04}$
Mg^{2+}	$59.5^{+0.4}_{-0.3}$	$8.4^{+0.4}_{-0.3}$	$26.9^{+0.6}_{-0.6}$	2.1E-03$^{+1.1E-03}_{-7.5E-04}$	8.4E-03$^{+4.2E-03}_{-6.7E-03}$	$0.71^{+0.08}_{-0.04}$	2.9E-03$^{+1.9E-03}_{-1.2E-03}$
Cl^-	$313.0^{+0.6}_{-0.6}$	$8.4^{+0.4}_{-0.3}$	$-52.4^{+0.5}_{-0.5}$	5.4E-04$^{+1.2E-04}_{-9.9E-05}$	8.4E-03$^{+4.2E-03}_{-6.7E-03}$	$0.91^{+0.03}_{-0.02}$	6.0E-04$^{+1.4E-04}_{-1.2E-04}$
ClO_4^-	$76.0^{+0.9}_{-0.6}$	$8.4^{+0.4}_{-0.3}$	$-59.1^{+1.0}_{-1.0}$	2.5E-03$^{+1.2E-03}_{-8.4E-04}$	8.4E-03$^{+4.2E-03}_{-6.7E-03}$	$0.91^{+0.03}_{-0.02}$	2.7E-03$^{+1.4E-03}_{-9.5E-04}$
NH_4^+	$-43.6^{+0.2}_{-0.4}$	$8.4^{+0.4}_{-0.3}$	$57.2^{+0.9}_{-0.9}$	3.9E-05$^{+3.6E-05}_{-2.8E-05}$	8.4E-03$^{+4.2E-03}_{-6.7E-03}$	$0.90^{+0.03}_{-0.02}$	4.3E-05$^{+4.2E-05}_{-3.2E-05}$
Sol-41 Sorceress-1 Cell 1 FU#018 Sample Addition							
Na^+	$37.8^{+2.7}_{-1.9}$	$5.7^{+1.7}_{-1.0}$	$49.9^{+0.9}_{-0.8}$	9.7E-04$^{+5.2E-04}_{-3.2E-04}$	1.9E-2$^{+2.7E-03}_{-1.7E-02}$	$0.88^{+0.02}_{-0.01}$	1.1E-03$^{+6.0E-04}_{-3.8E-04}$
K^+	$6.5^{+0.6}_{-1.1}$	$5.7^{+1.7}_{-1.0}$	$55.0^{+2.2}_{-2.1}$	1.4E-04$^{+1.8E-04}_{-8.4E-05}$	1.9E-2$^{+2.7E-03}_{-1.7E-02}$	$0.87^{+0.02}_{-0.01}$	1.7E-04$^{+2.0E-04}_{-9.8E-05}$
Ca^{2+}	$184.2^{+4.8}_{-5.5}$	$5.7^{+1.7}_{-1.0}$	$27.1^{+0.8}_{-0.7}$	2.6E-04$^{+4.4E-04}_{-1.8E-04}$	1.9E-2$^{+2.7E-03}_{-1.7E-02}$	$0.60^{+0.02}_{-0.02}$	4.2E-04$^{+7.6E-04}_{-3.1E-04}$
Mg^{2+}	$46.4^{+0.8}_{-0.5}$	$5.7^{+1.7}_{-1.0}$	$26.0^{+0.8}_{-0.8}$	1.4E-03$^{+1.2E-03}_{-6.3E-04}$	1.9E-2$^{+2.7E-03}_{-1.7E-02}$	$0.62^{+0.05}_{-0.01}$	2.2E-03$^{+2.0E-03}_{-1.1E-03}$
Cl^-	$312.3^{+4.3}_{-6.5}$	$5.7^{+1.7}_{-1.0}$	$-51.5^{+0.6}_{-0.5}$	2.4E-04$^{+1.2E-04}_{-1.1E-04}$	1.9E-2$^{+2.7E-03}_{-1.7E-02}$	$0.87^{+0.02}_{-0.01}$	2.4E-04$^{+1.3E-04}_{-1.1E-04}$
ClO_4^-	$70.2^{+3.0}_{-3.3}$	$5.7^{+1.7}_{-1.0}$	$-58.6^{+1.1}_{-0.9}$	1.8E-03$^{+1.0E-03}_{-7.4E-04}$	1.9E-2$^{+2.7E-03}_{-1.7E-02}$	$0.87^{+0.02}_{-0.01}$	2.1E-03$^{+1.2E-03}_{-8.6E-04}$
NH_4^+	$-13.0^{+2.3}_{-1.0}$	$5.7^{+1.7}_{-1.0}$	$56.1^{+1.6}_{-1.4}$	ND	N/A	N/A	ND
Sol-107 Sorceress-2 Cell 2 FU#022 Sample Addition							
Na^+	$84.8^{+1.8}_{-1.5}$	$10.0^{+0.1}_{-0.2}$	$51.3^{+1.0}_{-1.0}$	1.2E-03$^{+9.1E-04}_{-5.0E-04}$	2.6E-2$^{+6.9E-03}_{-2.4E-02}$	$0.86^{+0.04}_{-0.01}$	1.4E-03$^{+1.0E-03}_{-6.1E-04}$
K^+	$150.0^{+2.0}_{-0.8}$	$10.0^{+0.1}_{-0.2}$	$55.5^{+1.2}_{-1.2}$	3.3E-04$^{+2.6E-04}_{-1.4E-04}$	2.6E-2$^{+6.9E-03}_{-2.4E-02}$	$0.85^{+0.04}_{-0.01}$	3.9E-04$^{+3.2E-04}_{-1.7E-04}$
Ca^{2+}	$124.8^{+4.2}_{-4.2}$	$10.0^{+0.1}_{-0.2}$	$27.8^{+0.3}_{-0.3}$	3.4E-04$^{+4.0E-04}_{-1.8E-04}$	2.6E-2$^{+6.9E-03}_{-2.4E-02}$	$0.56^{+0.09}_{-0.03}$	6.0E-04$^{+7.9E-04}_{-3.4E-04}$
Mg^{2+}	$76.4^{+0.7}_{-0.6}$	$10.0^{+0.1}_{-0.2}$	$27.4^{+0.5}_{-0.6}$	2.2E-03$^{+1.6E-03}_{-8.8E-04}$	2.6E-2$^{+6.9E-03}_{-2.4E-02}$	$0.59^{+0.08}_{-0.03}$	3.7E-03$^{+3.0E-03}_{-1.7E-03}$
Cl^-	$313.7^{+1.7}_{-0.8}$	$10.0^{+0.1}_{-0.2}$	$-51.9^{+0.3}_{-0.4}$	4.0E-04$^{+1.7E-04}_{-8.2E-05}$	2.6E-2$^{+6.9E-03}_{-2.4E-02}$	$0.85^{+0.04}_{-0.01}$	4.7E-04$^{+2.1E-04}_{-1.1E-04}$
ClO_4^-	$111.6^{+2.1}_{-2.3}$	$10.0^{+0.1}_{-0.2}$	$-59.5^{+0.7}_{-0.7}$	1.8E-03$^{+8.7E-04}_{-6.6E-04}$	2.6E-2$^{+6.9E-03}_{-2.4E-02}$	$0.85^{+0.04}_{-0.01}$	2.2E-03$^{+2.2E-03}_{-8.1E-04}$
NH_4^+	$115.9^{+2.6}_{-2.0}$	$10.0^{+0.1}_{-0.2}$	$57.0^{+0.8}_{-0.8}$	2.2E-05$^{+5.0E-05}_{-2.8E-05}$	2.6E-2$^{+6.9E-03}_{-2.4E-02}$	$0.85^{+0.04}_{-0.02}$	2.6E-05$^{+6.0E-05}_{-3.2E-05}$

soil, under Mars ambient conditions, that produces a similar response. It is however, very unlikely.

[28] To generate a calibration curve that could be applied to the ISEs on Mars, a flight spare beaker and the payload system test bed (PST) electronics were initially calibrated with a set of solutions containing all the ionic species ranging from 10^{-5} to 10^{-2} M, identical to the preflight calibrations (TS20–24) [*Kounaves et al.*, 2009a]. All ISEs responded as they had previously during preflight calibrations. The calibration of the perchlorate ISE was then performed at 7°C by standard additions of $Mg(ClO_4)_2$ to the equivalent of the leaching solution plus the calibrant. As shown in Figure 7, both the Mg^{2+} and ClO_4^- ISEs gave responses with linear Nernstian slopes of −29 and −62 mV/decade, respectively. An extrapolation of the results down to the potential measured by the ClO_4^- ISE in the initial calibrant solution yielded a lower activity detection limit of 1.0×10^{-6} M for the WCL perchlorate sensors. (That is, there is no perchlorate in the calibration solution, so the potential of the ClO_4^- ISE in the calibration solution defines the lower detection limit.) This value was then substituted for the known activity of the ion in equation (2) to determine the calibration intercept. The activity of perchlorate in solution was then calculated using equation (3). An additional check of the calibration was validated on an additional flight-like beaker. The concentrations of the ClO_4^- are shown in Table 7.

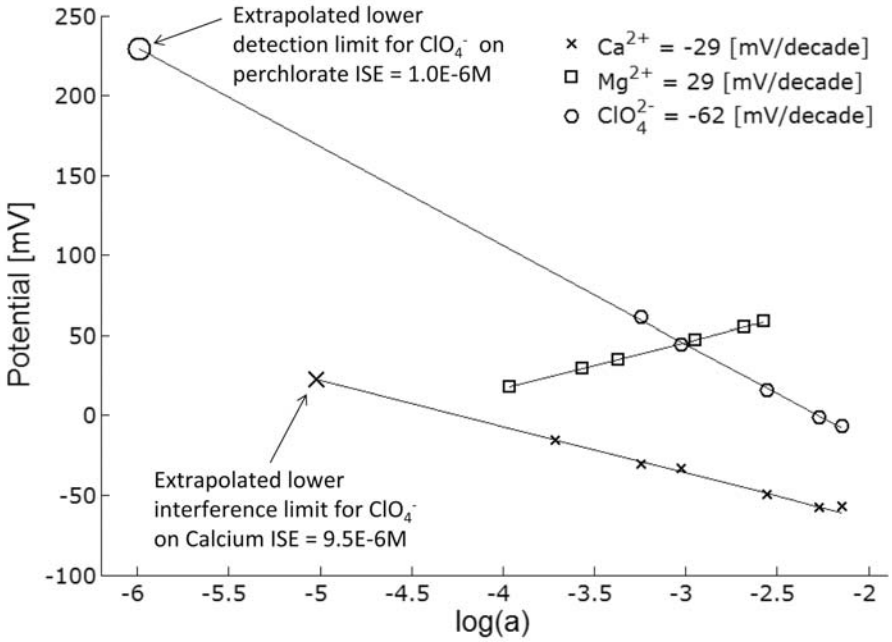

Figure 7. Calibration of the Hofmeister ISE (formally NO_3^- ISE) using standard additions of 0.5 M $Mg(ClO_4)_2$ into a calibrant equivalent solution (TS21). An extrapolation of the results yields the activity lower detection limit of 1.0×10^{-6} M for the WCL perchlorate sensors. The value is substituted in equation (2) to determine the calibration intercept.

4.4. Calibration and Determination of Calcium

[29] After the sample addition on Mars, a negative response of the potential for the Ca^{2+} ISE was observed. This response, in contrast to the positive potential change expected, has been shown to be due to the interference of the lipophilic perchlorate ion with complex formation in the ISE membrane [*Kounaves et al.*, 2003; *Lee et al.*, 2002]. This interference is unique to the calcium ISE, and causes a Nernstian decrease (−29 mV) in potential for every half decade increase in the activity of perchlorate. Since there was no perchlorate in the initial WCL calibration solutions it was necessary to find the lower limit of perchlorate that would interfere with the WCL calcium ISEs. This determination was performed by analyzing the response of the calcium ISE during the laboratory calibration of the perchlorate sensor described in the above section. The lower limit for the interference was determined by extrapolating the Nernstian decrease of the calcium ISE back to its calibration solution potential. This value corresponded to lower interference limit of 9.5×10^{-6} M ClO_4^- (That is, there is no interference of perchlorate on the calcium ISE in the initial calibration solution, and the potential of the calcium ISE in the calibration solution defines the lower interference limit.) The relative increase in interfering perchlorate as seen by the Ca^{2+} ISE is defined by the difference between this lower interference limit and the amount of perchlorate detected by the perchlorate ISE after sample addition. Accordingly, a correction for the Ca^{2+} ISE potential was calculated by multiplying the preflight calibration slope (mV/decade) of the calcium ISE by half of the logarithmic change in interfering perchlorate activity:

$$E_{Ca} = E_{CaOrig} - \left[S\left(\log\left(C_{ClO4-}\right) - \log\left(9.5 \times 10^{-6}\right)\right)/2\right] \quad (7)$$

where E_{Ca} is the corrected potential, E_{CaOrig} is the original potential, S is the slope, and C_{ClO4}^- is the concentration of the ClO_4^- determined by the ClO_4^- ISE. This correction provided an offset that was applied to the Ca^{2+} ISE potential. The methodology of section 4.2 was then applied to the corrected potential to obtain the activity and concentration.

[30] An additional calibration of Ca^{2+} to determine its response in the presence of perchlorate was preformed by standard addition of 1 M $CaCl_2$ with 4 mM $Mg(ClO_4)_2$ to a solution equivalent to the calibrant solution on Mars. The slope of the Ca^{2+} ISE correlated well with the initial calibration of the ISE in test solutions. Based on consistency of results, it was verified that it was appropriate to use the preflight calibrations for the ClO_4^- and Ca^{2+} ISEs were used to calculate their respective concentrations on Mars. Due to the presence of perchlorate, the Ca^{2+} ISE only shows Nernstian behavior from 1×10^{-5} to 1×10^{-3}M (Figure 8), but fortuitously includes the concentrations measured on Mars. The slope values for the calcium ISEs were determined from the preflight calibrations, and the intercepts were calculated by applying the method described above to the calcium signal once it was corrected for the interference of perchlorate.

4.5. Hydrogen Ion Concentration (pH)

[31] The three pH sensors (IrpH, pH1, and pH2) in each of the flight beakers were calibrated on Earth prior to beaker integration using four standard pH buffers. They were also calibrated after integration using the leaching solution saturated with (1) air and (2) air + 0.5% CO_2. The latter calibration, however, covered a very narrow calibration range (pH 5.0 to pH 6.5) and thus only the preintegration calibration is used for determining the pH.

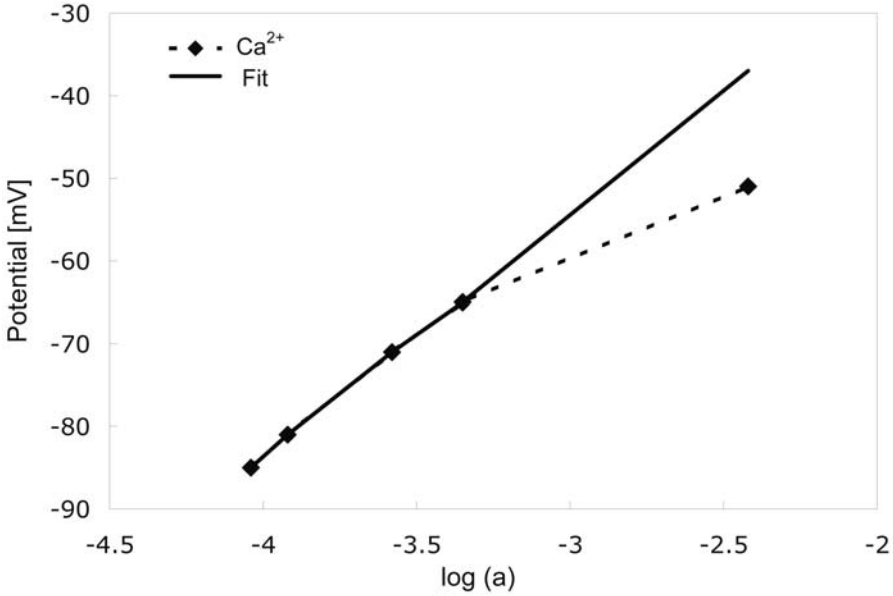

Figure 8. Calibration of Ca^{2+} in the presence of 8×10^{-3} M perchlorate by standard addition of 1 M $CaCl_2$. The response is Nernstian (29 mV/decade) only between 10^{-5} and 10^{-3} M.

[32] The calibration and determination of the solution pH on Mars requires knowledge of the partial pressure of the CO_2 (P_{CO2}) in the WCL beaker and tank headspace (Figure 1). The water tanks on the WCL flight units were loaded on Earth with the leaching solution that was equilibrated with a headspace gas mixture consisting of 0.8% CO_2, 94.2% N_2, and 5% He, at 1000 mbar pressure. The pH of this gas-saturated leaching solution, measured with an external pH electrode, was 5.14 at 22°C, as predicted by calculations. For the operating temperatures used on Mars, 1°C to 15°C, this corresponds to a range of pH 5.03 to 5.10 (0.0046 pH units/°C), respectively.

[33] After landing, the checkouts indicated that pressure in all four WCL cells had dropped to near zero. However, during the surface characterization phase the drawer on each WCL was opened and closed (''burped'') to the outside atmosphere for several seconds to allow the cell headspace to equilibrate with the Martian atmosphere. Cell 0 was burped on sol 5 and the rest of the cells were burped on sol 7. The external P_{CO2}, as measured by the MET station, was 8.4 mbar for those sols, the same as that of the water tank. Thus, after dispensing the leaching solution and prior to the first burp, the P_{CO2} in the beaker headspace would have been ~8.4 mbar and the solution at a known pH and temperature (Figure 9).

[34] During sample analysis the cell is burped several times. Since this occurs while the temperature of the solution is at or above the external boiling point, it may result in expulsion of the CO_2 from the cell headspace, limited only by the diffusion rate. Subsequently, CO_2 will evolve from the solution to reestablish equilibrium, raising the total pressure. Thus, the most accurate calibration point for the pH sensors is obtained after the leaching solution is dispensed but before any burps occur. Using this technique, a reliable calibration was achieved for the pH1 sensor in cell 0 (Rosy Red) and the pH1 and pH2 sensors in cell 1 (Sorceress 1). The measurements obtained with the pH sensors in cells 2 and 3 were unstable and either drifted significantly or had noise levels that were too high to allow the determination of an accurate calibration point.

[35] The parameters used for determining the pH are shown in Table 8. Figure 9 shows the response of the pH1 sensor for Sorceress 1 and the various points used to determine the pH. After selecting the calibration interval, the cell temperature was used to correct the preflight calibration slope. Equations (1) and (2) were then used to determine the hydrogen ion activity and pH. For the Rosy Red sample, the soil/solution mixture (1:25) gave a pH of 7.7(±0.3). For the Sorceress 1 sample, the pH 1 and pH 2 sensors gave a pH of 7.6(±0.3) and 7.6(±0.3), respectively. Taking the average of the Sorceress 1 pH as 7.6, and averaging with Rosy Red sample, gives an overall average pH of 7.7(±0.3). Using this calibrated pH value and the carbonate equilibrium likely dominating the solution, the P_{CO2} in the WCL headspace is calculated to be about 3 (±2) mbar.

4.6. Determination of Solution Electrical Conductivity

[36] In addition to the ion selective electrode potentials, each WCL cell measured electrical conductance (μS) at selected intervals during each experiment. Conversion of conductance to solution electrical conductivity (μS/cm) was made by multiplying the measured value by the cell constant values, obtained by averaging the results for the four preflight calibrations of each conductivity sensor. Table 9 shows the resulting specific conductivity for the soil solutions on Mars corrected to 25°C. For the salts identified on Mars, the correction used was 2.0% per 1°C [*Kounaves et al.*, 2009a].

[37] A significant uncertainty in the conductivity values arose from two issues. First, there were discrepancies between the expected and measured conductance in the

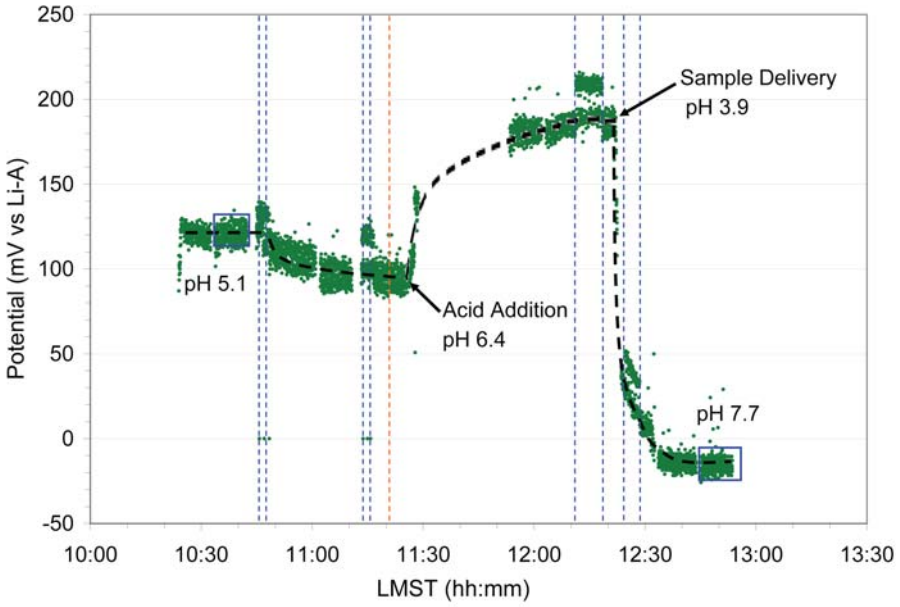

Figure 9. Response of the pH1 sensor for the Sorceress 1 soil sample on sol 41. The four pairs of dashed blue lines indicate the opening and closing of the drawer. The orange dashed line indicates the delivery of the crucible containing the calibrant. The blue boxes enclose the interval used to determine the initial calibration pH and the sample pH. LMST is the local mean solar time.

initial WCL leaching solution. The expected value for the conductance of the leaching solution corrected to 25°C was 82 μS, as determined from preflight calibrations, and the measured leaching solution conductance values for cells 1 and 2 corrected to 25°C were 102 μS and 116 μS, respectively. Accordingly, the lower uncertainty values in conductance were influenced by the choice of the ratio (actual conductance to measured conductance) used to scale it, 0.80 or 0.71, respectively. Second, uncertainties also arose from variations in the cell constant values calculated during the preflight calibrations and are reflected in the uncertainties for the cell constants in Table 9.

5. Discussion

[38] As can be seen in Figure 10 and Table 7, the three samples in cells 0, 1, and 2, gave within error similar concentrations for all ions. Within the resolution of the WCL measurements, this indicates the lack of any differences in the leachable portions between the surface sample and the two taken off the ice table at a depth of about 5 cm. The slightly lower concentrations for Sorceress 1 are most likely due to a smaller sample size of about 25%, which was evident in the before and after images of the drawer during delivery.

[39] As mentioned above, several attempts were made to deliver a sample to cell 3. In all cases it appears that even though soil filled the funnel, no significant amount made it into the solution. Cell 3 was thus effectively run as a blank. It is possible that the Golden Goose soil sample was devoid of salts. One could speculate that since the protected trough area may retain water and CO_2 ices for longer periods of time, during warmer periods, the water may either melt or form thin films that leach salts out of the top layers of soil. This does not seem likely though since the "slightly soluble" 3–5% calcite present in the soil [*Boynton et al.*, 2009] would have been difficult to totally leach out from the

Table 8. Values Used for Determination of pH[a]

ISE	Start Time (LMST)	End Time (LMST)	Potential (mV)	Temperature (°C)	Preflight Slope @T	Intercept (mV)
			Sol 30, Rosy Red, Cell 0, FU#020, Preburp			
pH1	1030:47	1034:49	$133.4^{+0.3}_{-0.8}$	$4.7^{+0.7}_{-0.7}$	$53.0^{+0.4}_{-0.4}$	$402.1^{+2.2}_{-2.7}$
			Sol 41, Sorceress 1, Cell 1, FU#018, Preburp			
pH1	1041:20	1043:06	$125.3^{+0.6}_{-0.5}$	$4.9^{+0.9}_{-1.0}$	$52.5^{+0.4}_{-0.4}$	$391.0^{+3.3}_{-5.5}$
pH2	1038:26	1043:06	$116.9^{+1.3}_{-0.9}$	$4.9^{+0.9}_{-1.0}$	$52.7^{+0.4}_{-0.4}$	$383.9^{+2.5}_{-3.5}$
ISE	Start Time (LMST)	End Time (LMST)	Potential (mV)	Temperature (°C)	Preflight Slope @T	pH
			Sol 30,Rosy Red, Cell 0, FU#020, Sample Addition			
pH1	1237:29	1246:26	$-13.7^{+1.0}_{-1.3}$	$8.4^{+0.4}_{-0.3}$	$53.7^{+0.3}_{-0.3}$	$7.74^{+0.11}_{-0.11}$
			Sol 41, Sorceress 1, Cell 1, FU#01, Sample Addition 8			
pH1	1243:37	1254:18	$-10.1^{+1.7}_{-3.1}$	$5.7^{+1.7}_{-1.0}$	$52.6^{+0.6}_{-0.4}$	$7.62^{+0.18}_{-0.12}$
pH2	1243:37	1254:18	$-17.7^{+0.6}_{-0.8}$	$5.7^{+1.7}_{-1.0}$	$52.8^{+0.6}_{-0.4}$	$7.61^{+0.12}_{-0.16}$

[a]LiB reference electrode was used for Rosy Red and LiA for Sorceress 1. P_{CO2} was assumed to be Mars ambient (8.4 mbar).

Table 9. Parameters Used for Determination of Solution Electrical Conductivity From Measured Conductance

Sample	Measured Sample Solution Conductance (μS) @ Temperature	Cell Constant (cm^{-1})	Temperature (°C)	EC at Temperature (μS/cm)	EC at 25°C (μS/cm)
Sol 30 Rosy Red	N/A	N/A	N/A	N/A	N/A
Sol 41 Sorceress 1	618^{+7}_{-124}	$1.51^{+0.17}_{-0.063}$	$5.7^{+1.7}_{-0.2}$	930^{+120}_{-220}	1370^{+200}_{-360}
Sol 107 Sorceress 2	882^{+20}_{-261}	$1.61^{+0.38}_{-0.16}$	$10.4^{+0.1}_{-1.0}$	1420^{+330}_{-520}	1900^{+510}_{-710}

Golden Goose soil by natural processes while leaving such high levels in the nearby Rosy Red soil.

[40] The solutions of all three samples are dominated by ClO_4^-, Mg^{2+}, and Na^+, at mM levels, with sub-mM concentrations of Ca^{2+}, K^+, and Cl^-. These ionic species are soluble components measured directly by the sensors, and may only represent a portion of the total amount of any specific chemical element present in the sample and/or solution. Except for sensor drift and other understood artifacts, the sensors did not measure any other soluble ionic species being released into the solution during the rest of the initial sol analysis for any of the samples.

[41] The discovery of about 3–5%(wt) calcite by TEGA in the soil [*Boynton et al.*, 2009], leads to the conclusion that the WCL soil/solution mixtures are saturated in at least $CaCO_3$. This suggest that the solution chemistry is most likely controlled by $CO_3^{2-} = HCO_3^-$, and CO_2 in a solution saturated with $CaCO_3$ and perhaps $MgCO_3$. Though this may not effect all ionic concentrations, the levels of Ca^{2+}, Mg^{2+}, the pH of the solution, and the effects of the CO_2 in the WCL headspace, are controlled by the carbonate system. This presents a challenge in determining the concentrations of the ionic species and the parent salts that may have been initially present before leaching of the sample. Identifying the parent salt(s) of the perchlorate may require additional evidence from TEGA or modeling. The implications for understanding the Martian chemistry may be different depending on the parent salt. A saturated solution of $Mg(ClO_4)_2$ versus $Na(ClO_4)_2$ would have a much lower freezing point, −70°C versus −30°C, respectively. Other implications for the discovery of carbonate and perchlorate have been previously discussed [*Hecht et al.*, 2009; *Boynton et al.*, 2009].

[42] Preliminary equilibrium models have been run using Geochemist's Work Bench (GWB) and the measured ionic composition of Rosy Red [*Kounaves et al.*, 2009b]. The results indicate a very complex system with the final species distribution dependent on several variables, including ionic strength, pH, precipitation, ion adsorption, the partial pressure of the CO_2, and the rate of equilibration. The models predict the measured concentrations for Ca^{2+}, Mg^{2+}, and pH, but do so with several possible compositions.

[43] Of the many models we have run to date, the one that gives the best fit to the WCL data includes (1) calcite and magnesite as solids with both $[Mg]_T$ and $[Ca]_T$ above saturation at 2×10^{-2}M, (2) the assumption that for the totally soluble ions (Na^+, K^+, Cl^-, and ClO_4^-) their total concentration is equal to the ionic concentration, as given in Table 7, (3) that the P_{CO2} in the WCL headspace is ~4 mbar at 7°C, and (4) electroneutrality. Under these conditions, the model gives a pH of 7.74 and an equilibrium value for the $[Mg^{2+}]$ and $[Ca^{2+}]$ of 3.5×10^{-3} M and 6.5×10^{-4} M, respectively. These concentrations are in good agreement with those given in Table 7 and their ratio (Mg/Ca) of 5.4 also agrees well with the average ratio calculated from Table 7 of 5.6. This indicates that the WCL solution may be saturated with both Ca and Mg carbonate. It is also possible that the Ca^{2+} and Mg^{2+} are also due to dissolution of solid solutions of $(Ca, Mg)CO_3$ as shown to exist in several of the Martian meteorites [*Bridges et al.*, 2001; *Ming et al.*, 2008].

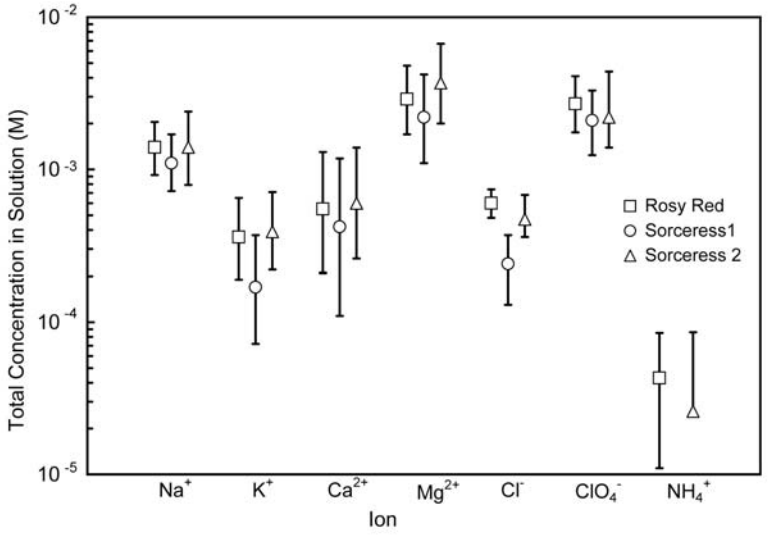

Figure 10. Concentration measured by all sensors for the three successfully delivered samples. Concentration is in mole/L after conversion from activity by applying equations (1)–(6).

[44] The models run provide guidance for further laboratory experiments with synthetic Mars samples. To differentiate between possible and plausible will require extensive formulation and testing with simulants and will allow a better prediction of the parent salts and formulation of a Mars simulant in high fidelity with that added to the WCL on Mars.

[45] **Acknowledgments.** We gratefully acknowledge the contribution of the many individuals associated with the Phoenix mission and the MECA Wet Chemistry Payload, particularly, John-Michael Morookian, Paula Grunthaner, Anita Fisher, Xiaowen Wen, Mark Weilert, Dick Morris, Casey Cable, Po-Chang Hsu, Emily Coombs, and the unwavering support of the Robotic Arm team who expertly acquired and documented our samples, and all the Phoenix engineers and staff that made it possible. The Phoenix mission was led by Peter Smith of the University of Arizona, Tucson, on behalf of NASA and was managed by NASA's Jet Propulsion Laboratory, California Institute of Technology, of Pasadena, California. The spacecraft was developed by Lockheed Martin Space Systems, Denver. We would like to thank Penny King (UNM) and Joel Hurowitz (JPL) for their review and the numerous suggestions they made that helped improve the manuscript.

References

Arvidson, R. E., et al. (2009), Results from the Mars Phoenix lander Robotic Arm experiment, *J. Geophys. Res.*, *114*, E00E02, doi:10.1029/2009JE003408.

Bibring, J.-P., and Y. Langevin (2008), Mineralogy of the Martian surface from Mars Express OMEGA observations, in *The Martian Surface: Composition, Mineralogy, and Physical Properties*, edited by J. F. Bell III, pp. 153–168, Cambridge Univ. Press, Cambridge, U. K.

Boynton, W. V., et al. (2009), Evidence for calcium carbonate at the Mars Phoenix landing site, *Science*, *325*, 61–64.

Bridges, J. C., D. C. Catling, J. M. Saxton, T. D. Swindle, I. C. Lyon, and M. M. Grady (2001), Alteration assemblages in Martian meteorites: Implications for near-surface processes, *Space Sci. Rev.*, *96*, 365–392, doi:10.1023/A:1011965826553.

Catling, D. C. (1999), A chemical model for evaporites on early Mars: Possible sedimentary tracers of the early climate and implications for exploration, *J. Geophys. Res.*, *104*, 16,453–16,469, doi:10.1029/1998JE001020.

Griffin, R. A., and J. J. Jurinak (1973), Estimation of activity coefficients from electrical conductivity, *Soil Sci.*, *116*, 26–30, doi:10.1097/00010694-197307000-00005.

Hecht, M. H., et al. (2009), Detection of perchlorate and soluble chemistry of the Martian soil; Findings from the Phoenix Mars Lander, *Science*, *325*, 64–67.

Hurowitz, J. A., S. M. McLennan, N. J. Tosca, R. Arvidson, J. R. Michalski, D. W. Ming, C. Schröder, and S. W. Squyres (2006), In situ and experimental evidence for acidic weathering of rocks and soils on Mars, *J. Geophys. Res.*, *111*, E02S19, doi:10.1029/2005JE002515.

King, P. L., D. T. Lescinsky, and H. W. Nesbitt (2004), The composition and evolution of primordial solutions on Mars, with application to other planetary bodies, *Geochim. Cosmochim. Acta*, *68*, 4993–5008, doi:10.1016/j.gca.2004.05.036.

Kounaves, S. P., et al. (2003), Mars Surveyor Program'01 Mars Environmental Compatibility Assessment Wet Chemistry Lab: A sensor array for chemical analysis of the Martian soil, *J. Geophys. Res.*, *108*(E7), 5077, doi:10.1029/2002JE001978.

Kounaves, S. P., et al. (2009a), The MECA Wet Chemistry Laboratory on the 2007 Phoenix Mars Scout Lander, *J. Geophys. Res.*, *114*, E00A19, doi:10.1029/2008JE003084.

Kounaves, S. P., et al. (2009b), Aqueous carbonate chemistry of the Martian soil at the Phoenix landing site, *Lunar Planet. Sci.*, *XL*, Abstract 2489.

Langevin, Y., P. Poulet, J.-P. Bibring, and B. Gondet (2005), Sulfates in the north polar region of Mars detected by OMEGA/Mars Express, *Science*, *307*, 1584–1586, doi:10.1126/science.1109091.

Lee, M. H., et al. (2002), Tweezer-type neutral carrier-based calcium-selective membrane electrode, *Anal. Chem.*, *74*, 2603–2607, doi:10.1021/ac011160b.

Ming, D. W., R. V. Morris, and B. C. Clark (2008), Aqueous alteration on Mars, in *The Martian Surface: Composition, Mineralogy, and Physical Properties*, edited by J. F. Bell III, pp. 519–540, Cambridge Univ. Press, Cambridge, U. K.

Quinn, R., and J. Orenberg (1993), Simulations of the Viking gas exchange experiment using palagonite and Fe-rich montmorillonite as terrestrial analogs: Implications for the surface composition of Mars, *Geochim. Cosmochim. Acta*, *57*, 4611–4618, doi:10.1016/0016-7037(93)90186-Z.

Shaw, A., R. E. Arvidson, R. Bonitz, J. Carsten, H. U. Keller, M. Lemmon, M. T. Mellon, M. Robinson, and A. Trebi-Ollennu (2009), Phoenix soil physical properties investigation, *J. Geophys. Res.*, *114*, E00E05, doi:10.1029/2009JE003455.

Smith, P. H., et al. (2008), Introduction to special section on the Phoenix Mission: Landing Site Characterization Experiments, Mission Overviews, and Expected Science, *J. Geophys. Res.*, *113*, E00A18, doi:10.1029/2008JE003083.

Smith, P. H., et al. (2009), H_2O at the Phoenix landing site, *Science*, *325*, 58–61.

Tosca, N. J., and S. M. McLennan (2006), Chemical divides and evaporite assemblages on Mars, *Earth Planet. Sci. Lett.*, *241*, 21–31, doi:10.1016/j.epsl.2005.10.021.

Tosca, N. J., S. M. McLennan, B. C. Clark, J. P. Grotzinger, J. A. Hurowitz, A. H. Knoll, C. Schröder, and S. W. Squyres (2005), Geochemical modeling of evaporation processes on Mars: Insight from the sedimentary record at Meridiani Planum, *Earth Planet. Sci. Lett.*, *240*, 122–148, doi:10.1016/j.epsl.2005.09.042.

W. V. Boynton, Lunar and Planetary Laboratory, University of Arizona, Tucson, AZ 85721, USA.

D. C. Catling, Department of Earth and Space Sciences, University of Washington, Seattle, WA 98195, USA.

B. C. Clark, Space Science Institute, 4750 Walnut St., Boulder, CO 80301, USA.

L. DeFlores and M. H. Hecht, Jet Propulsion Laboratory, California Institute of Technology, Pasadena, CA 91109, USA.

K. Gospodinova, Department of Mechanical Engineering, Massachusetts Institute of Technology, Cambridge, MA 02139, USA.

P. Hredzak, S. P. Kounaves, Q. Moore, J. Shusterman, S. Stroble, and S. M. M. Young, Department of Chemistry, Tufts University, Medford, MA 02155, USA.

J. Kapit, Woods Hole Oceanographic Institution, Woods Hole, MA 02543, USA.

D. W. Ming, NASA Johnson Space Center, 2101 NASA Pkwy., Houston, TX 77058, USA.

R. C. Quinn, SETI Institute, MS 239-4, Moffett Field, CA 94035, USA.

S. J. West, Invensys Process Systems, Foxboro, MA 02035, USA.